ELSEVIER

Thermochimica Acta 382 (2002) 189–198

thermochimica acta

www.elsevier.com/locate/tca

Biophysical investigations into the interaction of lipopolysaccharide with polymyxins

K. Brandenburg[a,*], I. Moriyon[b], M.D. Arraiza[b], G. Lewark-Yvetot[a], M.H.J. Koch[c], U. Seydel[a]

[a]*Research Center Borstel, Parkallee 10, 23845 Borstel, Germany*
[b]*Universidad de Navarra, Aptdo. 177, 31080 Pamplona, Spain*
[c]*European Molecular Biology Laboratory, Notkestr. 85, 22603 Hamburg, Germany*

Received 4 May 2001; received in revised form 7 June 2001; accepted 8 June 2001

Abstract

It is reported on the interaction of bacterial lipopolysaccharide (LPS, endo-toxin), having different sugar chain length covalently bound to its hydrophobic moiety lipid A, with the polycationic antibiotics polymyxin B (PMB) and PMB-nonapeptide (PMBN). The binding enthalpies and the lipid:peptide binding stoichiometries were determined by isothermal titration calorimetry (ITC). For LPS with a long sugar chain (S: smooth form LPS from *Yersinia enterocolitica*), the titration curves exhibit a strong exo-therm which can be interpreted to result from the electrostatic interaction of the negative charges of the LPS with the positive charges of the peptides. In contrast, the titration curves of LPS with a short sugar chain (LPS Re from *Escherichia coli*) and of free lipid A yield complex patterns of endo- and exo-therms, which result from the superposition of electrostatic binding, fluidization of the acyl chains and a transition between different three-dimensional aggregate structures of the endo-toxins due to peptide binding. Infrared spectroscopy indicates that the fluidizing effect of the polymyxins is similar for both types of LPS and for lipid A. Small-angle X-ray diffraction reveals, however, that the Re-type LPS and lipid A are converted from a cubic into a multilamellar structure, whereas, the S-form LPS transforms from a unilamellar into a multilamellar structure with a small number of lamellae. The presented data allow a better understanding of the interaction of peptides with endo-toxin molecules. © 2002 Elsevier Science B.V. All rights reserved.

Keywords: Lipopolysaccharides; Peptide binding; Isothermal titration calorimetry; Fluidization; Reaggregation

1. Introduction

Lipopolysaccharides (LPS) represent the main amphiphilic component of the outer leaflet of the outer membrane of Gram-negative bacteria and are called endo-toxins due to their ability to induce a variety of biological effects in mammals, in particular, the production of proinflammatory cytokines [1]. At low endo-toxin concentrations, the biological effects may be beneficial, since cytokines such as tumor-necrosis-factor-α (TNF-α) have been shown to possess anti-tumor activity. At higher endo-toxin concentrations, however, the release of cytokines leads to self-poisoning of the body, eventually resulting in septic shock syndrom [2].

LPS consist of a sugar portion with varying length of oligo- or polysaccharide chains depending on the kind of bacterial mutant—rough mutant LPS Re to Ra

* Corresponding author. Tel.: +49-4537-188235; fax: +49-4537-188632.
E-mail address: kbranden@fz-borstel.de (K. Brandenburg).

0040-6031/02/$ – see front matter © 2002 Elsevier Science B.V. All rights reserved.
PII: S0040-6031(01)00731-6

or smooth form LPS—which is covalently linked to the hydrophobic moiety of LPS, lipid A, which anchors the LPS molecule to the membrane. Lipid A is composed of a diglucosamine backbone which is phosphorylated in positions 1 and 4′ and acylated by 6 to 7 hydrocarbon chains ester- and amide-linked in positions 2,3 and 2′, 3′ in the case of enterobacterial strains [3]. For LPS from other bacterial genera, the lipid A structure may differ in particular with respect to the acylation pattern: for LPS from *Y. enterocolitica* O:8; for example, the main species in the lipid A moiety may be a tetraacylated [4] or pentaacylated compound [5], and non-stoichometric amounts of other lipid species may be present. For deep rough mutant LPS Re, two very unusual sugars 2-keto-3-deoxyoctonate (Kdo) are linked to the lipid A moiety, each of which has one carboxylate group. Thus, the LPS backbone of all different kinds of bacterial mutants carries a high number of negative charges.

On the basis of these structural prerequisites, it may not be surprising that polycationic drugs (peptides, proteins, and/or antibiotics) such as polymyxin B (PMB) may effectively protect against the pathophysiological effects of LPS [6–11]. The innate immune system also provides various cationic proteins such as lactoferrin, the defensins, the CAP family, and bactericidal permeability-increasing protein (BPI, [7,8]) to combat against whole bacteria as well as isolated LPS. A variety of studies describes the effects of PMB on outer membranes of intact bacteria as well as on isolated LPS or anionic phospholipids [12–16]. A systemic application of PMB is, however, severely restricted by its toxicity at higher concentrations. It has been found that the nonapeptide PMBN—a deacylated derivative of PMB—is essentially nontoxic and also lost the bactericidal action, but it still binds to LPS. It sensitizes various pathogenic bacterial strains against the direct bactericidal effect of human serum [11,17–19].

The detailed study of the interaction of drugs with target structures such as LPS requires the application of a variety of physical techniques. One of them is isothermal titration calorimetry (ITC), which allows to determine binding constants and binding stoichiometry. In the frame of a biophysical study on the PMB- and PMBN-interaction with LPS from various—pathogenic and nonpathogenic—strains we observed titration curves which were most readily interpretable for LPS with long sugar chain, but exhibited a complex, not readily interpretable course for deep rough mutant LPS and free lipid A.

For an interpretation of ITC data, it has to be taken into account that cationic drugs do not only interact electrostatically with the negatively charged groups such as the phosphates, but also interact with the hydrophobic region. This may lead to a change in acyl chain fluidity and a reorientation of the aggregate structure. These processes should be dependent on the precise chemical structure of LPS, i.e. its acylation pattern within the hydrophobic region (lipid A) and the different sugar chain lengths in the various rough mutants and smooth forms.

To characterize these processes in more details, we have—beside ITC—applied Fourier-transform infrared (FTIR) spectroscopy for an elucidation of the $\beta \leftrightarrow \alpha$ acyl chain melting behaviour and small-angle X-ray scattering (SAXS) using synchrotron radiation for the determination of the aggregate structure. It was found that at least three processes superimpose in the interaction of PMB with the endo-toxins: fluidization of the acyl chains, reorientation of the aggregate structure, and electrostatic binding of PMB essentially to the negatively charged groups (carboxylates, phosphates).

Comparison of the results with those obtained for free lipid A allows a qualitative interpretation of the ITC data of endo-toxin binding to PMB: the endothermic processes dominating at the beginning of the titration of LPS Re and lipid A are caused by reaggregation and fluidization. At higher PMB concentration, the exo-thermic process is solely due to electrostatic binding of PMB to the negative charges.

2. Materials and methods

LPS from the deep rough mutant Re *E. coli* Jc7623 strain WBB01 (kindly provided by W.Brabetz, Forschungszentrum Borstel) was extracted from bacteria grown at 37 °C by the phenol/chloroform/petrol ether method [20], purified, and lyophilized. LPS from *Y. enterocolitica* WA 289 O:8 was obtained from bacteria grown in standard tryptic soy broth (TSB) at 37 °C [5].

Free lipid A was isolated from LPS Re by acetate buffer treatment. After isolation, the resulting lipid A

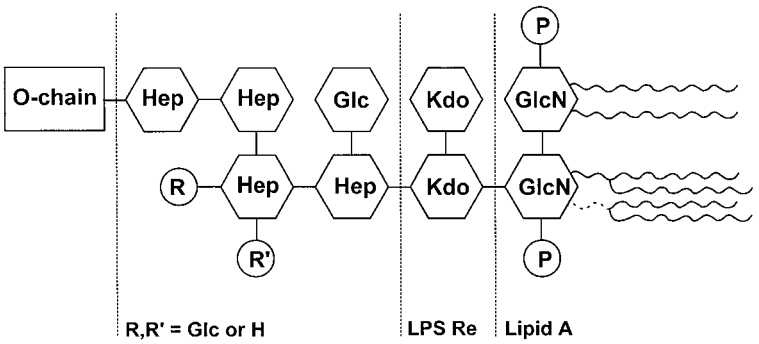

Fig. 1. Schematic chemical structure of LPS from *Y. enterocolitica* O:8 (S-type LPS) and from *E. coli* WBB01 (Re-type LPS) and the hydrophobic moiety of LPS, lipid A. The lipid A is hexaacylated in *E. coli*-type LPS [3], in the heterogeneous *Y. enterocolitica* LPS, the main species of lipid A is pentaacylated (unpublished results). The O-chain typical for smooth form LPS usually consists of a polymer of a repeating unit of an oligosaccharide [1], the main species of *Y. enterocolitica* contains only one unit.

was purified and converted to the triethylamine salt form.

The known chemical structure of lipid A from LPS Re was checked by the analysis of the amount of glucosamine, total and organic phosphate, and the distribution of the fatty acid residues applying standard procedures. The amount of Kdo was also checked and in no case exceeded 5%. The chemical structures of the investigated LPS are given in Fig. 1.

2.1. Sample preparation

The lipid samples were usually prepared as aqueous dispersions at high buffer (20 mM Hepes) content, depending on the sensitivity of the technique: 0.05 mM for the ITC experiment, 5 mM for the infrared, and 40 mM for the X-ray experiment. In all cases, the lipids were suspended directly in buffer and temperature-cycled several times betwen 5 and 70 °C and then stored at least 12 h before measurement.

2.2. Isothermal titration calorimetry (ITC)

Microcalorimetric experiments of peptide binding to endo-toxins were performed on an MCS isothermal titration calorimeter (Microcal Inc., Northampton, MA, USA) at 37 °C. After thorough degassing of the suspensions, the endo-toxin samples (5×10^{-5} M) were filled into the microcalorimetric cell (volume 1.3 ml) and the peptides (5×10^{-4} M) into the syringe compartment (volume 100 μl). After temperature equilibration, the peptides were titrated in 5 μl portions in every 10 min into the endo-toxin-containing cell, under constant stirring, and the heat of interaction after each injection measured by the ITC instrument was plotted versus time. A control measurement in which the peptide was titrated into pure buffer solution indicated that the heat of dilution was negligible. The total heat signal from each experiment was determined as the area under the respective single peaks and plotted versus the [peptide]:[endo-toxin] molar ratio. Since the instrument works in temperature equilibrium at a constant 'current feedback' corresponding to a power of approximately 74 μW, exo-thermic reactions reduce the current and endo-thermic ones increase it. All titration curves were repeated at least four times.

2.3. FTIR spectroscopy

The infrared spectroscopic measurements were performed on an FTIR spectrometer IFS-55 (Bruker, Karlsruhe, Germany). The lipid samples were placed in a CaF_2 cuvette separated by a 12.5 μM thick teflon spacer. Temperature scans were performed automatically in the range 10–70 °C with a heating rate of 3 K/5 min. In every 3 K, 50 interferograms were accumulated, apodized, Fourier transformed, and converted to absorbance spectra.

For strong absorption bands, the evaluation of the band parameters (peak position, band width, and band intensity) was performed with the original spectra, if

necessary after subtraction of the strong water bands allowing the determination of the position of the peak maxima with a precision of better than 0.1 cm^{-1}.

Here, in particular, the symmetric stretching vibration of the methylene groups is evaluated, the band position of which is a measure of lipid order [21].

2.4. X-ray diffraction

X-ray diffraction measurements were performed at the European Molecular Biology Laboratory (EMBL) outstation at the Hamburg synchrotron radiation facility HASYLAB using the double-focusing monochromator-mirror camera X33 [22]. Diffraction patterns in the range of the scattering vector $0.07 < s < 1\,nm^{-1}$ ($s = 2\sin\Theta/\lambda$, 2Θ scattering angle and λ the wavelength [0.15 nm]) were recorded at 37 °C with exposure times of 2 or 3 min using a linear detector with delay line readout [23]. The wavelength calibration was done with tripalmitate as a standard having a periodicity of 4.06 nm at room temperature. Further details of the data acquisition and evaluation system can be found elsewhere [24]. In the diffraction patterns presented here, the logarithm of the diffraction intensities log $I(s)$ is plotted against the scattering vector s. The X-ray spectra were interpreted according to procedures described previously [25] which allow to assign the spacing ratios of the main scattering maxima to defined three-dimensional structures. The lamellar and cubic structures which are particularly relevant here can be characterized by the following features:

1. *Unilamellar*: The reflections are very broad and do not show sharp diffraction maxima.
2. *Multilamellar*: The reflections are sharp and grouped in equidistant ratios, i.e. at 1, 1/2, 1/3, 1/4, etc. of the lamellar repeat distance d_l.
3. *Cubic*: These are non-lamellar three-dimensional structures. Their various space groups differ in the ratio of their spacings. The relation between reciprocal spacing $s_{(hkl)} = 1/d_{(hkl)}$ and lattice constant a is ((hkl) = Miller indices of the respective set of plane)

$$S_{(hkl)} = \frac{\sqrt{h^2 + k^2 + l^2}}{a}$$

3. Results and discussion

Isothermal titration calorimetric experiments are presented for LPS from the pathogenic strain *Y. enterocolitica* TSB and for the LPS Re from *E. coli* WBB01 (chemical structures in Fig. 1) and for the peptides PMB and PMBN. The original ITC curves for LPS from *Y. enterocolitica* TSB—0.15 mM in 1.3 ml—to which PMBN was added—titration steps 3 μl of a 3 mM solution—are shown in Fig. 2. A strong exothermic reaction takes place already at the beginning of the titration for each injection of the peptide and saturation occurs after nearly 20 titration steps (100 min).

This exo-thermic reaction can be interpreted to result from electrostatic binding of the positively charged groups of PMBN to negatively charged groups, in particular to the lipid A phosphates, which are known to be binding sites for polycationic peptides [26]. In Fig. 3, the enthalpy changes measured calorimetrically are plotted versus the peptide:LPS ratio for PMB and PMBN. Given the number of negative (4 in the lipid) and positive (5 in PMB and 4 in PMBN) charges, compensation is expected to take place at a molar ratio of [peptide] : [LPS] = 0.8 or 1.0, respectively. Fig. 3 illustrates that an excess of the peptides is necessary to neutralize all negative charges suggesting

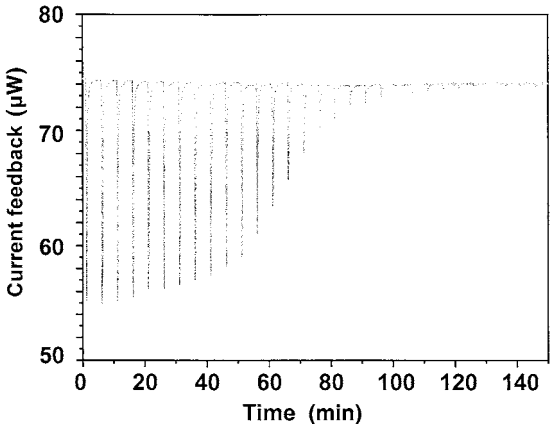

Fig. 2. Isothermal calorimetric titration of LPS from *Y. enterocolitica* O:8 (0.15 mM) with polymyxin nonapeptide PMBN (3 mM). For this, the 1.3 ml LPS dispersion in the calorimetric cell was titrated in every 5 min with 3 μl of the peptide. The reduction of the current feedback indicates the occurrence of an exo-thermic reaction.

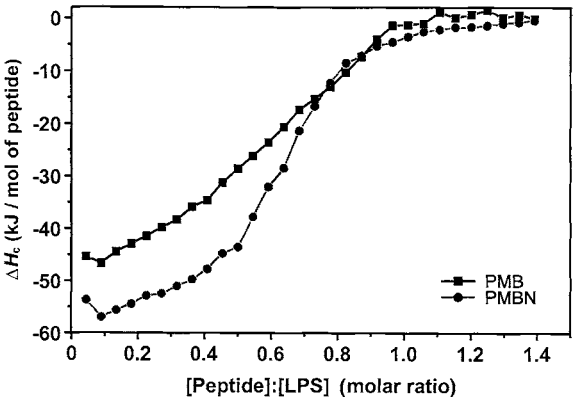

Fig. 3. Enthalpy change of the LPS-protein reaction versus [peptide]:[LPS] molar ratio for LPS from *Y. enterocolitica* O:8 and the peptides PMB and PMBN from calorimetric titration curves as shown in Fig. 2. Binding saturation can be estimated to lie in the range of molar ratios 1.1–1.2.

that not all charges of LPS are readily accessible for the peptides due to sterical hindrance within the aggregates.

In contrast to this behaviour, the titration of LPS Re from *E. coli* with the peptides (Fig. 4) is much more complex. In the first part of the titration curve for PMB, a clear endo-thermic reaction takes place with a maximum at a ratio [PMB]:[LPS] of 0.1 and a constant enthalpy change in the range between 0.3 and 0.6 molar. At a ratio of 0.7, the reaction converts into an

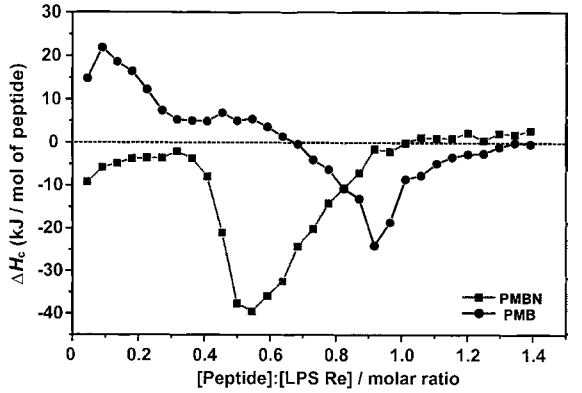

Fig. 4. Enthalpy change of the LPS-protein reaction versus [peptide]:[LPS] molar ratio for LPS from *E. coli* WBB01 and the peptides PMB and PMBN from calorimetric titration curves as shown in Fig. 2. Binding saturation can be estimated to lie in the range of molar ratios 1.2–1.3.

exo-thermic one which runs into saturation at [PMB] : [LPS] = 1.2–1.3 molar. A similar complex titration is found for PMBN. Note, however, that similarly to the data for the *Yersinia*-LPS saturation of peptide:LPS binding lies around 1.0 (PMBN) to 1.2 (PMB).

For an interpretation of these effects, it has to be taken into account that peptide binding to LPS may not solely consist of binding of the cationic peptide to the negative charges of LPS. Changes of the LPS assembly (for example in the mobility of the acyl chains and/or in the supramolecular aggregate structure) may also occur and contribute to the enthalpy changes. To quantitatively elucidate these effects, the acyl chain mobility was determined by Fourier-transform infrared (FTIR) spectroscopy and the aggregate structure by synchrotron radiation SAXS.

$\beta \leftrightarrow \alpha$ acyl chain melting of LPS Re was monitored as function of temperature in the presence of varying amounts of PMB and PMBN from changes of the symmetric stretching vibrational band $\nu_s(CH_2)$ of the methylene groups (Fig. 5a,b). Clearly, in the absence of the peptides LPS Re undergoes a transition from an ordered (gel phase, β) with the band position lying at 2850 cm^{-1} to an unordered (liquid crystalline phase, α) with the band position lying around 2852.5 cm^{-1} [27]. Above a [LPS]:[PMB] molar ratio of 1:0.15, PMB induces a significant increase of the wavenumber values corresponding to a fluidization of the hydrocarbon chains. Similar effects are found for PMBN (Fig. 5b).

The aggregate structures for various LPS:peptide mixtures at high water content and 37 °C were monitored by applying synchrotron radiation SAXS. The diffraction patterns—the logarithm of the scattering intensity is plotted versus the scattering vector *s* which is proportional to the scattering angle—indicate for pure LPS Re (Fig. 6a) in the absence of the peptides a complex aggregate structure with non-lamellar characteristics which was shown in former investigations to represent an inverted cubic structure [28]. In the presence of the peptides (b–d), the patterns become characteristic for lamellar structures—reflections at equidistant ratios. From Fig. 6, it can be deduced that at molar ratios [LPS] : [PMB] = 1 : 0.25, still some non-lamellar structures are present, which convert completely at an equimolar content of LPS and PMB (c). Interestingly, PMBN induces two different

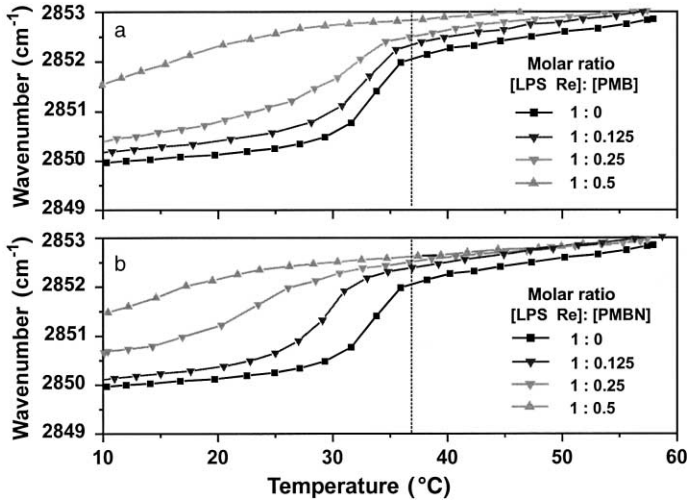

Fig. 5. Gel to liquid crystalline ($\beta \leftrightarrow \alpha$) phase transition of the acyl chains of LPS from *E. coli* WBB01 at different concentrations of PMB: (a) and PMBN, (b) from the peak position of the symmetric stretching vibration of the methylene groups lying at 2850 cm^{-1} in the gel phase and at 2852.5 cm^{-1} in the liquid crystalline phase, respectively [23].

superimposed lamellar structures corresponding to periodicities of 7.50 and 6.37 nm (Fig. 6d).

The absence of the complex effects seen for mixtures of LPS Re and the peptides in the titration curves of the LPS from *Y. enterocolitica* and PMBN indicates that for this LPS the effects due to fluidization and reaggregation may differ from those for LPS Re. FTIR spectroscopic data show, however, that also for LPS from *Y. enterocolitica* the addition of PMB ([LPS]:[PMB] 1:0.4 molar) leads to an increase of the wavenumber at 37 °C from 2852.3 to 2852.8 cm^{-1} (data not shown), a quantitatively identical fluidization. In contrast to this, SAXS data indicate a quite different aggregate structure for LPS from *Y. enterocolitica* as compared to LPS Re (Fig. 7a). The broad diffraction maximum centered around 6.94 nm can be

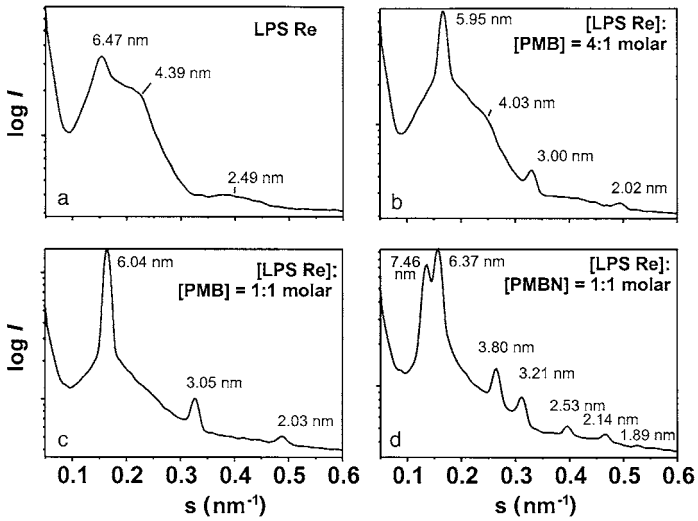

Fig. 6. X-ray diffraction patterns of LPS from *E. coli* WBB01 in the absence (a) and presence of PMB (b, c) and PMBN (d) at 90% water content and 37 °C. Presented is the logarithm of the scattering intensity log I versus the scattering vector $s = 2 \sin \Theta / \lambda$.

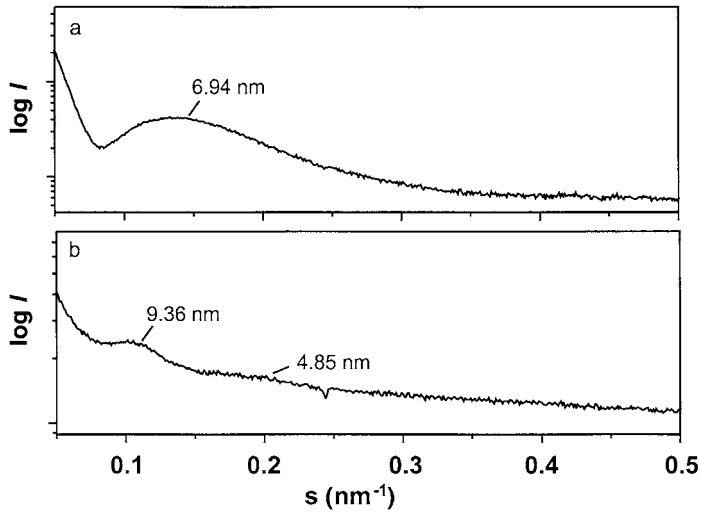

Fig. 7. X-ray diffraction patterns of LPS from *Y. enterocolitica* O:8 in the absence (a) and presence (b) of PMB at 90% water content and 37 °C. Presented is the logarithm of the scattering intensity log I versus the scattering vector $s = 2 \sin \Theta / \lambda$.

interpreted as resulting from a unilamellar structure. This structure changes only slightly into a multilamellar structure in the presence of an equimolar content of LPS and PMB (Fig. 7b) as deduced from the occurrence of the two reflections (first and second order). The lacking sharpness of the reflections indicates the presence of only a low number of lamellae and, therefore, only a slight reorientation of the LPS assembly following peptide binding.

Accordingly, the diffraction patterns change only marginally upon addition of the peptides. The chemical structure of the *Yersinia*-LPS shows some heterogeneity, but the lipid A moiety mainly consists of a pentaacyl compound and of a Ra-type core structure with a short O-antigen unit (see Fig. 1).

The two LPS are identical with respect to their number of negative charges (4), and, accordingly, display a similar binding saturation characteristics. Therefore, free lipid A from *E. coli* lacking the two Kdo moieties of LPS Re which thus carries only two negative charges of the phosphates was also investigated.The results from the three different techniques are plotted in Fig. 8A–C. The ITC measurements again exhibit a rather complex behaviour, starting with a strong endo-thermic reaction followed by an exo-therm which reaches saturation at $[\text{PMB}] : [\text{lipid A}] = 0.4$ molar (Fig. 8A). This ratio corresponds to the exact charge compensation of the two compounds. In contrast, the IR experiment (Fig. 8B) indicates that the fluidizing effect of PMB goes far beyond this ratio: although the ITC curve of Fig. 8A does not indicate any change beyond a ratio of 0.4, the fluidizing action of PMB can be observed at least up to an equimolar ratio. The action of PMB on the aggregate structure of lipid A (Fig. 8C) is similar to that of LPS Re: in absence of PMB a cubic inverted structure (a) which converts to a multilamellar structure with equidistant reflections upon addition of PMB (b–d).

These data suggest that a finer differentiation between the three effects should be possible. The transition from a cubic into a multilamellar aggregate structure apparently causes a calorimetric endo-therm counterbalancing the exo-therm due to electrostatic binding. So far, no data are available with respect to the enthalpy change of the Q ↔ L transitions. A value of 3 kJ/mol has been reported for the L ↔ H_{II} transition of the phospholipid 1-palmitoyl-2-oleoyl-phosphatidylethanolamine [29]. This value is too low to explain the present results—assuming that these different systems are at all comparable. Further complications may arise from the observation of a drastic dependence of the binding enthalpy for peptide-vesicle binding on phospholipid vesicle size, ranging from −30 kJ/mol for small vesicles (‘enthalpy-driven’) to + 4 kJ/mol for larger vesicles (‘entropy-driven’)

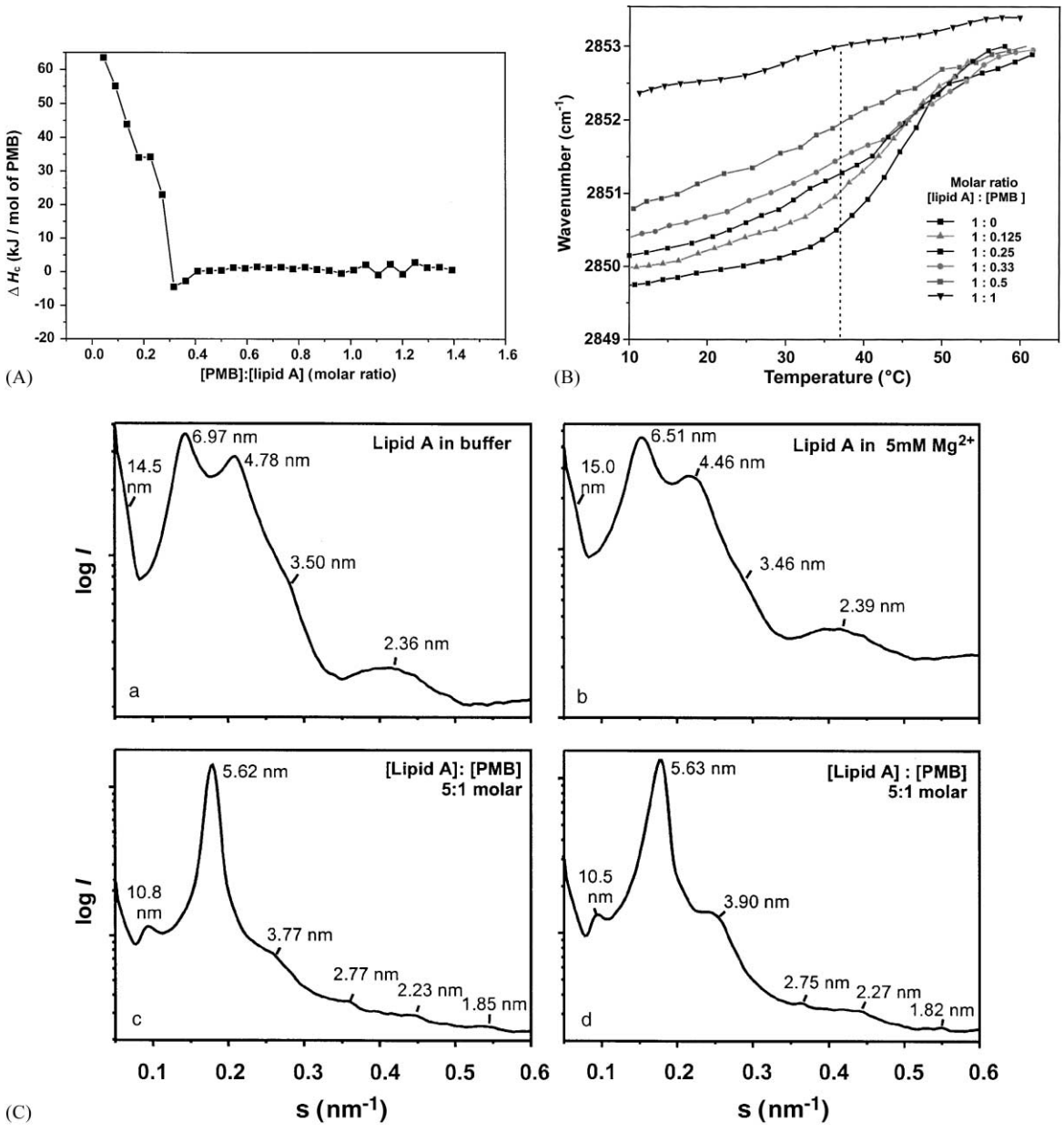

Fig. 8. (A) Enthalpy change of the LPS-peptide reaction versus [peptide]:[lipid A] molar ratio from the LPS of *E. coli* WBB01 and PMB determined from calorimetric titration curves as shown in Fig. 2. Binding saturation can be estimated to lie at a molar ratio 1:0.4. (B) Gel to liquid crystalline ($\beta \leftrightarrow \alpha$) phase transition of the acyl chains of lipid A isolated from the LPS of *E. coli* WBB01 at different concentrations of PMBdetermined from the peak position of the symmetric stretching vibration of the methylene groups. (C) X-ray diffraction patterns of lipid A from the LPS of *E. coli* WBB01 in buffer: (a), on 5 mM Mg (b), in the presence of PMB in buffer (c), in the presence of PMB in 5 mM Mg (d), at 90% water content and 37 °C. Presented is the logarithm of the scattering intensity log I versus the scattering vector $s = 2 \sin \Theta / \lambda$.

[30]. It will be, therefore, the aim of future experiments to characterize these dependences.

Fluidization should also be an endo-thermic process. This can be deduced from previous differential scanning calorimetry (DSC) on the $\beta \leftrightarrow \alpha$ phase transition of rough mutants LPS form *E. coli* and *Salmonella minnesota*, for which a value of 30 kJ/mol was found [31]. An estimate of the enthalpy change attributable to the fluidity change taking into account that there is a change of 0.7 cm in wavenumber value (Fig. 8B) between [lipid A]:[PMB] 1:0–1:0.33 molar, corresponding to approximately to 1/3 of the whole phase transition, yields enthalpy changes negligible as compared to the enthalpies measured in the present investigation.

As a model for the interaction of PMB with isolated endo-toxins, we propose a two-step mechanism: in the first step, the negative charges (phosphates, carboxylates) of the LPS and lipid A samples bind electrostatically to the positive charges of PMB or PMBN. In the second step, for LPS with a short sugar chain and for lipid A, an increase in fluidity of their hydrocarbon chains takes place which is connected with a dramatic reorientation of the aggregate structure. This process is accompanied by a hydrophobic interaction of PMB due to the insertion of its small acyl chain. This model is in accordance with the data presented by Koch et al. [16], who found—also with ITC—a strong exo-therm ($\leq$60 kJ/mol), and also proposed an electrostatic association as the first step and penetration of PMB into the LPS membrane as second step. However, they found for an LPS Re from *E. coli* an 'ideal' titration curve similar to our data for the LPS with the longer sugar chains (Fig. 2). Since their LPS Re should be expected also to adopt an inverted cubic structure in the absence of PMB, this discrepancy cannot readily be understood. The only likely explanation is presently that these authors used 50 mM Tris–HCl buffer instead of the Hepes buffer used here.

In contrast to our data and also to those of Koch et al are the ITC data performed by Srimal et al. [32] and Thomas and Surolia [33] with PMB and a series of different lipid A and LPS structures. The authors found the binding of the peptide to the endo-toxin samples to be non-cooperative and endo-thermic, from which they proposed a predominantly hydrophobic interaction between PMB and the lipids as driving force, and the electrostatic interaction playing only a minor role. The measuring temperature could play a key role in the explanation of this discrepancy, since these authors performed their ITC measurements at non-physiological temperatures in the range 6–25 °C for LPS and 10–31 °C for lipid A, i.e. clearly below the T_c for the respective lipids. A comparison is further hampered by the use of a different buffer (50 mM sodium phosphate buffer). Anyway, their interpretation seems to be improbable not only in the light of our finding, but also in those of other authors. For example, the fact that in PMB-resistant bacterial mutants, the negative charges are compensated by an increasing amount of positive charges within the headgroup region of LPS emphasizes the importance of the electrostatic interaction [34,35].

Pristovsek and Kidric [36] studied the influence of PMB-binding on the conformation of LPS aggregates with NMR and molecular modeling.They propose that the detoxification of the polymyxins is caused by breaking up the supramolecular structure of the lipid A moiety of LPS that is connected with its toxic action, an interpretation which is in excellent accordance to the data presented here, a cubic structure corresponding to an active and the lamellar one to an inactive conformation [37].

Our data indicate a great similarity in the behaviour of PMB and PMBN in all tests (Figs. 3–6) despite considerable differences in biological systems (e.g. PMB is bactericidal and PMBN not). It is important to note that the mode of action of the peptide against outer membranes of bacteria is different from that against LPS aggregates. PMB produces transient pores (lesions), whereas, PMBN does not [14]. In a subsequent step, the PMB can penetrate the bacterial cell via these lesions ('self-promoted uptake') [15].

The presented data should contribute to an understanding of the ability of PMBN to sensitize bacteria [17–19] with respect to the action of other drugs. As deduced from Fig. 5, PMBN leads to a strong fluidization comparable to that by PMB. Sensitization may be understood on the basis of the reduced packing density of the lipid A moiety allowing the drug molecules to penetrate the membrane via the hydrophobic pathway.

4. Conclusions

The present results indicate for the first time that binding of the polycationic peptides PMB and PMBN

with bacterial endo-toxin consists of a superposition of at least three different effects, the electrostatic binding, a fluidization of the acyl chains of the endo-toxins, and the reaggregation of the latter molecules. The extent of the singular effects depends on the number of negative charges within the endo-toxins and on the length of its sugar side chain.

In further experiments, we will extend these studies by analysing also LPS and lipid A from PMB-resistent strains such as *Proteus mirabilis* R45 and *Salmonella typhimurium* mutants [34,35].

Acknowledgements

We thank G. von Busse for performing IR spectroscopic measurements. This work was supported by the Deutsche Forschungsgemeinschaft (SFB 367, project B8 and BR 1070/2-1) and by a PIUNA grant from the University of Navarra.

References

[1] U. Mamat, U. Seydel, O. Holst, D. Grimmecke, E.T. Rietschel, in: B.M. Pinto (Ed.), Carbohydrates and Their Derivatives Including Tannins, Cellulose, and Related Lignins, Elsevier, Amsterdam, 1999, pp. 179–240.
[2] E.T. Rietschel, U. Mamat, L. Hamann, A. Wiese, L. Brade, P. Sanchez-Carballo, T. Mattern, P. Zabel, D. Heumann, F. Di Padova, S. Hauschildt, A. Woltmann, Novo Acta Leopoldina 307 (1999) 93.
[3] U. Zähringer, B. Lindner, E.T. Rietschel, in: D.C. Morrison, H. Brade, S. Opal, S. Vogel (Eds.), Endo-toxin in Health and Disease, Marcel Dekker, New York, 1999, pp. 93–114.
[4] C. Oertelt, B. Lindner, M. Skurnik, O. Holst, Eur. J. Biochem 268 (2001) 554.
[5] J.A. Bengoechea, R. Díaz, I. Moriyon, Infect. Immun. 64 (1996) 4891.
[6] R.E.W. Hancock, The Lancet 349 (1997) 418.
[7] M.G. Scott, R.E.W. Hancock, Crit. Rev. Immunol. 20 (2000) 407.
[8] K. Bush, M. Macielag, Curr. Opin. Chem. Biol. 4 (2000) 433.
[9] M. Schindler, M.J. Osborn, Biochemistry 18 (1979) 4425.
[10] M. Teuber, J. Bader, Arch. Microbiol. 109 (1976) 51.
[11] M. Vaara, Microbiol. Rev. 56 (1992) 395.
[12] W. Hartmann, H.J. Galla, E. Sackmann, Biochim. Biophys. Acta 510 (1978) 124.
[13] P. Kubesch, J. Boggs, L. Luciano, G. Maass, B. Tümmler, Biochemistry 26 (1987) 2139.
[14] G. Schröder, K. Brandenburg, L. Brade, U. Seydel, J. Membr. Biol. 118 (1990) 161.
[15] A. Wiese, M. Münstermann, T. Gutsmann, B. Lindner, K. Kawahara, U. Zähringer, U. Seydel, J. Membr. Biol. 162 (1998) 127.
[16] P.-J. Koch, J. Frank, J. Schüler, C. Kahle, H. Bradaczek, J. Colloid Interf. Sci. 213 (1999) 557.
[17] M. Vaara, T. Vaara, Nature 303 (1983) 526.
[18] M. Vaara, FEMS Microbiol. Lett. 18 (1983) 117.
[19] F. Rose, K.U. Heuer, U. Sibelius, S. Hombach-Klonisch, L. Kiss, W. Seeger, F. Grimminger, J. Infect. Dis. 182 (2000) 191.
[20] C. Galanos, O. Lüderitz, O. Westphal, Eur. J. Biochem. 9 (1969) 245.
[21] K. Brandenburg, S. Kusumoto, U. Seydel, Biochim. Biophys. Acta 1329 (1997) 193.
[22] M.H.J. Koch, J. Bordas, Nucl. Instrum. Method 208 (1983) 461.
[23] A. Gabriel, Rev. Sci. Instrum. 48 (1977) 1303.
[24] C. Boulin, R. Kempf, M.H.J. Koch, S.M. McLaughlin, Nucl. Instrum. Method A249 (1986) 399.
[25] K. Brandenburg, W. Richter, M.H.J. Koch, H.W. Meyer, U. Seydel, Chem. Phys. Lipids 91 (1998) 53.
[26] D.C. Morrison, D.M. Jacobs, Immunochemistry 13 (1976) 813.
[27] K. Brandenburg, S.S. Funari, M.H.J. Koch, U. Seydel, J. Struct. Biol. 128 (1999) 175.
[28] K. Brandenburg, M.H.J. Koch, U. Seydel, J. Struct. Biol. 108 (1992) 93.
[29] M.R. Wenk, J. Seelig, Biochim. Biophys. Acta 1372 (1998) 227.
[30] G. Beschiaschvili, J. Seelig, Biochemistry 31 (1992) 10044.
[31] K. Brandenburg, A. Blume, Thermochim. Acta 119 (1987) 127.
[32] S. Srimal, N. Surolia, S. Balasubramanian, A. Surolia, Biochem. J. 315 (1996) 679.
[33] C.J. Thomas, A. Surolia, FEBS Lett. 445 (1999) 420.
[34] K. Nummila, I. Kilpeläinen, U. Zähringer, M. Vaara, I.M. Helander, Mol. Microbiol. 16 (1995) 271.
[35] I.M. Helander, I. Kilpeläinen, M. Vaara, Mol. Microbiol. 11 (1994) 481.
[36] P. Pristovsek, J. Kidric, J. Med. Chem. 42 (1999) 4604.
[37] U. Seydel, A.B. Schromm, R. Blunck, K. Brandenburg, in: R.S. Jack (Ed.), CD14 in the Inflammatory Response, Karger, Basel, 2000, pp. 5–24.